Remote Sensing of Environment 114 (2010) 637–646

Contents lists available at ScienceDirect

Remote Sensing of Environment

journal homepage: www.elsevier.com/locate/rse

Landsat TM/ETM+ and tree-ring based assessment of spatiotemporal patterns of the autumnal moth (*Epirrita autumnata*) in northernmost Fennoscandia

Flurin Babst [a,b,*], Jan Esper [a,c], Eberhard Parlow [b]

[a] Dendro Sciences Unit, Swiss Federal Research Institute WSL, Switzerland
[b] Institute for Meteorology, Climatology and Remote Sensing, University of Basel, Switzerland
[c] Institute of Geography, University of Mainz, Germany

ARTICLE INFO

Article history:
Received 26 July 2009
Received in revised form 14 October 2009
Accepted 15 November 2009

Keywords:
Digital change detection
Dendroecology
Forest disturbances
Insect outbreaks
Defoliation
Betula pubescens

ABSTRACT

We used fine-spatial resolution remotely sensed data combined with tree-ring parameters in order to assess and reconstruct disturbances in mountain birch (*Betula pubescens*) forests caused by *Epirrita autumnata* (autumnal moth). Research was conducted in the area of Lake Torneträsk in northern Sweden where we utilized five proxy parameters to detect insect outbreak events over the 19th and 20th centuries. Digital change detection was applied on three pairs of multi-temporal NDVI images from Landsat TM/ETM+ to detect significant reductions in the photosynthetic activity of forested areas during disturbed growing seasons. An image segmentation gap-fill procedure was developed in order to compensate missing scan lines in Landsat ETM+ "SLC-off" images. To account for a potential dependence of local outbreak levels on elevation, a digital elevation model was included in the defoliation recognition process. The resulting damage distribution map allowed for the assessment of outbreak intensity and distribution at the stand level and was combined with tree-ring data and historical documents to produce a multi-evidence outbreak detection. Defoliation events in the tree-ring data were recognized as significant deviations from temperature related growth.

Our outbreak detection scheme allowed for the reconstruction of nine major insect outbreaks over the past two centuries. The reconstruction proved reliable but only robust for severe defoliation events. Low-intensity incidents were not captured.

1. Introduction

Rejuvenation is crucial for forested ecosystems in order to ensure their continuity and resilience against extreme impacts (e.g. Esper & Schweingruber, 2004). In Fennoscandia, where mountain birch (*Betula pubescens*) is the predominant tree species forming the treeline (Tenow et al., 2004), defoliation caused by geometrids such as *Epirrita autumnata* (autumnal moth) is among the most important ecological disturbances resulting in growth reduction and tree mortality (Tenow, 1972). *Epirrita* has a univoltine life cycle and its larvae hatch at the time of budbreak in the host forests (Bylund, 1997). The potential population growth rate is very high (six to ten fold in one generation) and in northern Scandinavia, the moths tend to reach outbreak numbers every 9–10 years in the middle of each decade (Bylund, 1995). Similar regular outbreak patterns may be found in most forest Lepidoptera species that reach outbreak levels (e.g. gypsy moth, Haynes et al., 2009). Cycles are regional and may become synchronized if conditions are similar. They do not, however, spread from an epicentre but occur simultaneously in different localities (Ruohomäki et al., 2000; Klemola et al., 2006). To reach outbreak level, at least three consecutive years of population growth are needed (Virtanen et al., 1998). Moreover, the population dynamics of *E. autumnata* are strongly dependant on the frequency of lethal minimum winter temperatures. Egg-killing temperatures are below −35.1 to −36.5 °C in high winter and −28.3 to −29.8 °C in early spring (Tenow & Nilssen, 1990). Thus, the distribution and the disturbance regimes in northern Fennoscandia are likely to be altered by regional climate change. Compared to the current state, the forest area protected by cold is predicted to decrease to 1/3 by 2050 and to 1/10 by 2100 (Virtanen et al., 1998).

Over the past two decades, various efforts have been made to assess insect-related disturbances and their consequences in forested ecosystems using remote sensing and related methodologies (e.g. winter moth, Hogda & Tommervik, 1998; jack pine budworm, Radeloff et al., 2000; Leckie et al., 2005; gypsy moth, Townsend et al., 2004; Johnson et al., 2006; pine sawfly, Solberg et al., 2006; Eklundh et al., 2009; mountain pine beetle, Wulder et al., 2006). Early studies commonly determined the spatial properties of population peaks and classified single satellite images to detect outbreak ranges (e.g. Franklin & Raske, 1994). In contrast, recent investigations have

* Corresponding author. Dendro Sciences Unit, Swiss Federal Research Institute WSL, Switzerland.
E-mail address: flurin.babst@wsl.ch (F. Babst).

0034-4257/$ – see front matter © 2009 Elsevier Inc. All rights reserved.
doi:10.1016/j.rse.2009.11.005

applied digital change detection techniques such as image differencing, principal component analysis on multi-temporal remote sensing data (see Radeloff et al., 1999 for a summary). Temporal analysis has either focused on changes in the forest distribution (Masek, 2001) or assessed insect outbreaks using time series analysis on annual areal survey information (Johnson et al., 2006).

In the mountain birch forests of northern Fennoscandia, most satellite-based research has focused on tree cover mapping and forest dynamics (e.g. Seppälä & Rastas, 1980; Heiskanen & Kivinen, 2007). Spatiotemporal analyses of *E. autumnata* infestations (Tømmervik et al., 2001) are sparse. Thus, other methodologies such as laboratory experiments (e.g. Hoogesteger & Karlsson, 1992), dendrochronology (e.g. Eckstein et al., 1991) or detailed analyses of climate proxies (Ruohomäki et al., 2000; Jepsen et al., 2008) have been important for the assessment of forest disturbance in this region. These, however, provide no area-wide information about intensity and distribution of defoliation during *Epirrita* population peaks.

In this study, we use fine-spatial resolution remotely sensed satellite data to assess the spatial distribution and intensity of the three most recent *Epirrita* outbreaks in the area of Lake Torneträsk (Swedish Lapland) in 1986, 1994 and 2004 (Karlsson et al., 2004). Digital change detection was applied to determine decreases in photosynthetic activity during *Epirrita* outbreak events. Fine-spatial resolution satellite imagery was then combined with tree-ring data. Dendroecological techniques have often been used in the past to assess the temporal aspects of forest Lepidoptera outbreaks (e.g. *Zeiraphera diniana*, Esper et al., 2007; *E. autumnata*, Eckstein et al., 1991). This multi-evidence approach was used to establish a spatiotemporal link between the area-wide spectral and in-situ tree-ring data. It is, to our knowledge, the first reconstruction of insect outbreak events where satellite-based digital change detection is supported by natural proxy data.

2. Materials and methods

2.1. Study area

To guarantee the comparability with previous research on *E. autumnata* population peaks (e.g. Tenow, 1972; Eckstein et al., 1991; Bylund, 1995; Karlsson et al., 2004), this study was carried out in the area of Lake Torneträsk (68°19′6″N, 19°16′44″E; 341 m a.s.l.) and the Abisko National Park in Swedish Lapland (Fig. 1). The region of interest is situated in a mountainous area on the eastern slope of the Scandes Range, which retains moisture that is brought from the Atlantic Ocean by cyclones following the main westerly air-flow (Tenow, 1972). As a consequence of this lee situation, average precipitation is only 304 mm per year of which 124 fall during summer. Nevertheless, water is not a limiting factor for tree growth as transpiration is low due to the cold temperatures. The average annual air temperature is −0.6 °C and mean summer temperature (JJA) is 10 °C allowing tree growth up to an elevation of about 650 m a.s.l. Climate data used in this is study derived from the Abisko Scientific Research Station (ANS), which is situated at the southern margin of Lake Torneträsk at an elevation of 385 m a.s.l. Its consistent time series reaches back until 1913.

The productivity of the forest mainly depends on temperature during the main growing season, which lasts from the beginning of June to the end of August (Eckstein et al., 1991). The lower areas are covered by a monocultural mountain birch forest of the heath-type. At most slopes above the lake, the denser meadow birch forest prevails (Vegetationskarta, 1981). Field observations showed that where drier ecological conditions prevail locally, particularly on hills, the area-wide birch forest is occasionally interrupted by coniferous trees, mainly Scots Pine (*Pinus sylvestris*). Scots Pine is not affected by the leaf-eating caterpillars of *E. autumnata* (Ruohomäki & Haukioja, 1992).

Artificial surface structures may directly affect the dispersal of the poor-flying moths (Ruohomäki et al., 2000). There are no major settlements around Lake Torneträsk or the adjacent areas which had to be taken into account during the georeferencing process. Small villages are concentrated on the south side of the main lake along the road and the railroad from Kiruna (SWE) to Narvik (NOR). Summer and winter tourism in the Abisko National Park is limited to the main trails and a small skiing resort. The north shore is mainly unsettled.

2.2. Digital change detection

Fine-spatial resolution satellite imagery is useful for studying changes in land cover and in the magnitude of peak greenness over time (e.g. Stow et al., 2004; Fraser et al., 2005). Many previous studies

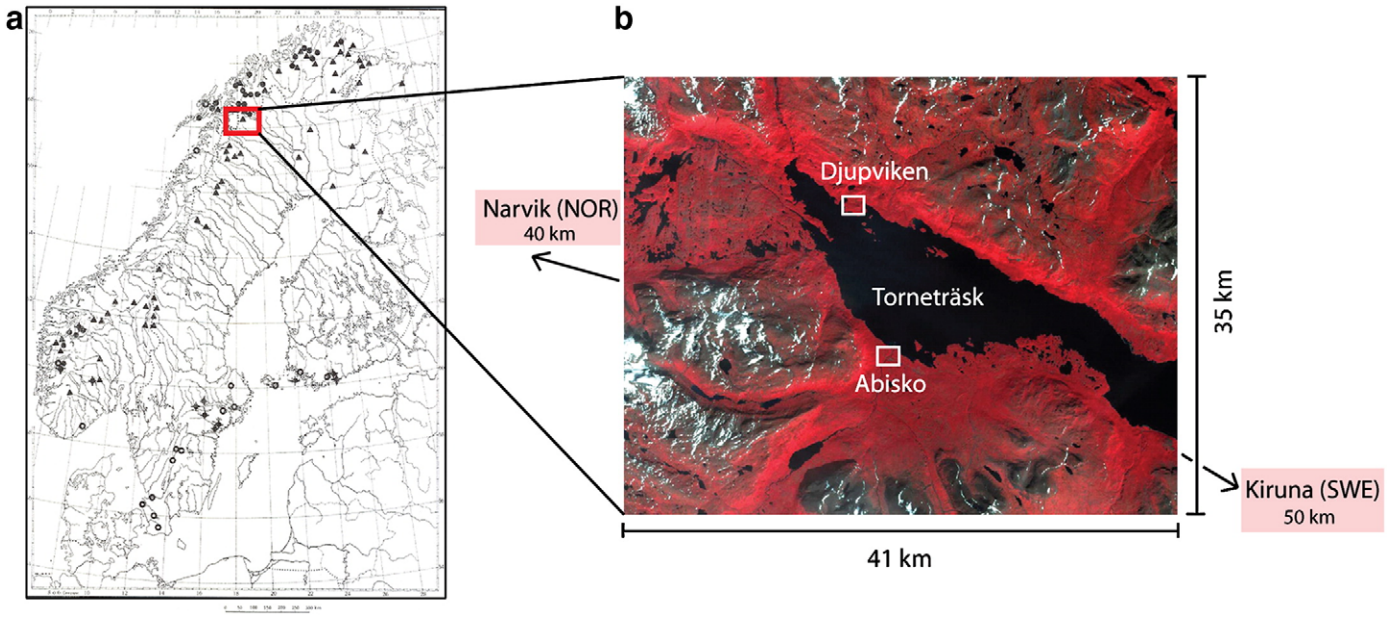

Fig. 1. Location of the research area: (a) distribution of documented insect outbreaks along the Scandes (*O. brumata*, *O. fagata*, *O. autumnata*; Tenow, 1972); (b) false-colour infrared composite of the spatial subset that has been used for all satellite-based investigations. (For interpretation of the references to colour in this figure legend, the reader is referred to the web version of this article.)

have shown that when images from the same season and location in different years are compared, a significant decline in the normalized difference vegetation index (NDVI) is associated with vegetation disturbance patterns (e.g. Remmel & Perera, 2001). This is the case if the phenology does not change significantly between the comparison years and if the leafy canopy is replaced by soil or vegetation with a low photosynthetic rate (Jin & Sader, 2005). Both conditions are fulfilled in our study area (Tenow, 1972).

Two pairs of satellite images covering the 1986 and 1994 *Epirrita* outbreaks in the research area (Karlsson et al., 2004) originated from Landsat TM; two more images of Landsat ETM+ were used to detect the disturbance patterns during the most recent event in 2004 (Table 1). Tree-ring data were collected from sampling plots of approximately 200 m^2. Thus, Landsat imagery is suitable for a direct comparison with ring-width data since its spatial resolution in the visible (VIS) and near infrared (NIR) spectral bands (Table 1) allows for the detection of NDVI changes on a sub-site level (stand level).

An additional scene recorded by the Indian Remote Sensing Satellite (IRS, see Table 1) in the damage-free year 1998 was included as a basis for masking out the forested areas. Its LISS-III (Linear Imaging Self Scanner) sensor has a spatial resolution of 23 m in all four spectral bands (Richards & Xiuping, 1999). All seven images were pre-processed and registered to the Swedish RT90 map coordinates that were extracted from a digitized version of the Topografisk Fjällkartan (Sheet BD6, 1:100,000).

In addition to the two-dimensional information, a digital elevation model (DEM, spatial resolution 50 m) developed at the Institute for Meteorology, Climatology and Remote Sensing of the University of Basel was included in order to assess the topographical (vertical) component of the damage distribution. The correctness of its coordinates was ensured by computing an exposition map and a visual comparison of the location of fixed points such as mountain peaks to the Landsat images and the IRS scene.

A supervised surface classification was applied to the image of the undisturbed summer of 1990 using a maximum likelihood algorithm. This classification method was chosen since it is most suitable for training sites with a large spectral variance like the ones defined in the diffuse forest–heath transition zone (Jensen, 2005). It was used to extract surface features such as lakes. These were later transformed into suitable masks for better clearness and interpretation of the damage distribution map. Preceding irradiation (e.g. Song et al., 2001) was corrected using the relatively simple approach of spectral band ratios (Holben & Justice, 1981). Because of its much larger wavelength, the thermal band was excluded. Due to the low solar zenith angle at high latitudes, steep mountains create shadows even in mid-summer. Some of these were misclassified as lakes and had to be omitted from the lake mask. This was achieved via the slope angle data layer which strictly allowed lakes for horizontal slopes only.

The arbitrary selection of training sites for three different vegetation density classes did not allow for their transformation into an accurate forest mask. Instead, a threshold NDVI value was iteratively determined, based on the 1998 (attack-free) IRS image. The computed forest area has been verified based on size and geographic coordinates using a digitized version of the 1981 Vegetation map. This was done under the assumption that the forested area did not change significantly between 1981 and 1998 (Masek, 2001). Despite the challenge that transition between Fjäll-heath and mountain birch forest is not always discrete, an NDVI value of 0.45 was found to correctly represent the border of the forested area (Vegetationskarta, 1981). The resulting forest mask could be applied on all three image pairs under the reasonable assumption that forest borders did not change significantly over the research period (Masek, 2001).

Optimal results of digital change detection require image pairs that are taken on the same day of the year to avoid biases induced by differences in illumination or changes in the vegetation period (Coppin et al., 2002). Here, the maximum time difference between the available comparison images was 22 days. In order to quantify a possible NDVI variation caused by this time offset, two MODIS images (spatial resolution 250 m) from the equivalent dates of the attack-free year were used. Only a minor shift of NDVI values of −0.04 which was not consistent over the study area was registered. This led to the conclusion that digital change detection could be applied without further pre-treatment of the three image pairs.

Various change detection techniques, each with their own strengths and weaknesses, are compared and summarized in Rogan et al. (2002) and Lu et al. (2004). Of these, principal component analysis (PCA), which was originally designed to transform large datasets into much smaller sets of uncorrelated variables (Jensen, 2005), was applied. Using a layer stacking algorithm on the Landsat image pairs, one multi-date NDVI image was created for each of the three *Epirrita* outbreaks in 1986, 1994 and 2004. A standardized PCA was carried out on each of them maintaining the same number of bands. The correlation matrix which was used to calculate the eigenvalues has the advantage that each band was forced to have equal weight in the derivation of the new component images (Eastman & Fulk, 1993). When analysing the output, the first principal component (PC1) which contains the majority of variance (depending on the outbreak intensity, e.g. 67% for the 2001/2004 image pair) found in the original data set (Li & Yeh, 1998) was interpreted as the common signal of the two bands. PC2 contained the information that is different in both layers which is equal to the NDVI change in forested areas between the two multi-temporal bands. The results were verified using image differentiation (not shown here) on the same multi-temporal image pairs (Williams, 1995; Masek, 2001).

In May 2003, Landsat ETM+ suffered a failure of the Scan Line Corrector (SLC). The valid parts of the following "SLC-off" images have normal radiometric and geometric quality while wedge-shaped gaps appear that are equal to a data loss of 22% (Trigg et al., 2006, Fig. 2). For the purpose of this study, these gaps could not be filled with information from earlier "SLC-on" images since the missing scan lines in the 2004 image would have been be filled with information from non-outbreak years (Maxwell et al., 2007). This would greatly bias the aspired damage detection. Neither is it feasible to assume that the defoliation pattern remains constant over the missing scan lines (ten pixels). Thus, interpolation cannot be applied directly on the PC2 band as a gap-fill solution. If, however, a certain generalization is achieved by calculating density slice classes and producing segmentation images, it is plausible to assume that the pixels of the missing scan line belong to the same damage class as those in the neighbouring segment (Wulder et al., 2004). By applying this modified version of the multi-segment model by Maxwell et al. (2007), who applied a gap-fill algorithm on coincident spectral data derived from earlier Landsat ETM+ "SLC-on" images, the gaps in the 2004 damage distribution map based on Landsat ETM+ were successfully filled.

Table 1
Satellite images used to assess three outbreak periods of *Epirrita autumnata*. The spatial resolution is shown for bands 1–5, 7 and for band 6/band 8 in brackets (Parlow, 1985; Goward et al., 2003).

Index	Scene outbreak year	Scene outbreak-free year	Satellite source	Spectral bands	Spatial resolution
1	07/29/2004	08/20/2001	Landsat-7 (ETM+)	8	30 m (60 m/15 m)
2	09/03/1994	08/23/1996	Landsat-5 (TM)	7	30 m (120 m)
3	07/20/1986	07/15/1990	Landsat-5 (TM)	7	30 m (120 m)
4		08/31/1998	IRS	4	23 m

2.3. Tree-ring and climate data

Based on the 2004 damage distribution information derived from digital imaging, two sampling transects each with three sites at

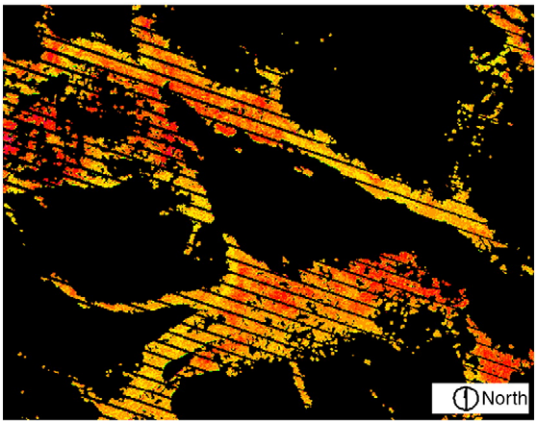

Fig. 2. Unclassified second principal component (PC2) containing missing scan lines due to the SLC failure of Landsat ETM+ in 2003. The 2004 result is displayed for forested areas only. Red colours indicate heavy defoliation whereas yellow colours indicate less severe NDVI reductions. The gap-filled damage detection is shown in Fig. 4. (For interpretation of the references to colour in this figure legend, the reader is referred to the web version of this article.)

different elevations (low, middle, top) were defined in order to assess the effect of defoliation on radial growth and to reconstruct major outbreaks further back in time than covered by satellite imagery. Transect 1 (T1) is located at the east-facing slope above the village of Abisko, south of Lake Torneträsk. T2 was set on the south-facing slope above Djupviken at the north-eastern end of the lake. An additional mountain birch site (R; Table 2) which was found to have been undamaged during the three most recent outbreaks based on the digital change detection scheme and was selected as a reference. Via GPS-derived coordinates and the digital elevation model, the sampling sites could be directly linked to the results of the change detection.

At each site, increment cores from 18–20 trees were taken during a field campaign in summer 2008. In order to deal with the naturally high risk for missing rings in mountain birch (Takaoka, 1993) and to account for the substantial growth variance of 80.9% between the stems of a polycormic individual (Karlsson et al., 2004), four cores per tree were sampled to ensure correct dating. All pre-treatments and measurements of the collected samples were carried out in the Dendro Sciences Laboratory of the Swiss Federal Research Institute WSL. The resulting annual tree-ring-width (TRW) series were crossdated (Fritts, 1976) using COFECHA software (Holmes, 1983) to ensure correct dating and develop reliable site chronologies. Smoothing splines (Cook & Peters, 1981) of 50 years length were used to remove low-frequency trends (e.g. age trend) while short-term variations in radial growth were preserved. This was done using the program ARSTAN (Cook & Holmes, 1986) with a variance adjustment (Cook & Peters, 1997) run in advance in order to avoid biases due to replication and cross-correlation changes during the calculation of arithmetic means (Frank et al., 2007). This way, a total of seven standardized site chronologies were developed (Table 2) that represent radial tree growth along T1 and T2.

Table 2
Inventory of the series included in the site chronologies (minimum replication 3 trees) along T1, T2 and in R. Length of the chronologies with a replication >5 trees. R-bar and EPS are measures of inter-tree coherence (see Wigley et al., 1984) and were calculated based on the average series of all trees included in the chronologies and over the period of chronology length. Furthermore, the number of individual radii (increment cores) included in the site chronologies is displayed.

Site	Length of chronology	R-bar	EPS	Number of trees	Number of radii (main-stem)	Number of radii (side-stem)
T1_low	1915–2007	0.67	0.93	13	46	13
T1_mid	1820–2007	0.53	0.91	12	30	18
T1_top	1970–2007	0.71	0.97	17	66	21
T2_low	1931–2007	0.71	0.94	11	26	3
T2_mid	1862–2007	0.59	0.92	15	35	1
T2_top	1855–2007	0.49	0.92	22	40	4
R	1877–2007	0.59	0.92	10	25	1

For the study area, representative climate data is produced at the ANS (Abisko Scientific Research Station) whose consistent time series reaches back until 1913. We calculated residuals between the six birch site chronologies and three sources of reference data: instrumental temperature data (*T*), a ring-width chronology from a reference mountain birch site (R), and a maximum latewood density chronology derived from Scots Pine (P). A large portion (48–60%) of the variance in age-corrected mean ring-width series from high-latitude forests can be directly related to June–August (JJA) temperature. Together with growth variations between individual trees, 80% of ring-width variability can be explained (Karlsson et al., 2004). This allows significant deviations from temperature-determined growth to be interpreted as disturbances.

The chronologies of sites T1_mid, T2_mid and R reach further back in time than the available climate time series from the ANS. We therefore used a nearby maximum latewood density chronology derived from Scots Pine (*P. sylvestris*) (Frank et al. in prep.) as a proxy for regional growing season temperature variations (Schweingruber, 1988; Eschbach et al., 1995) prior to 1913. Over the overlapping period (1913–2006), this chronology correlates highly ($r = 0.71$) with instrumental growing season temperature data and is therefore a suitable substitute for the pre-instrumental period.

R and P strongly correlate with instrumental JJA temperature ($r = 0.62$ and 0.71 respectively).

R (1887–2007) was derived from the same species as the sites along T1 and T2 and is likely to react similarly to climate variations. This site, however, was selected based on digital change detection and is therefore only guaranteed to be outbreak-free back to 1986. Scots Pine on the other hand is a non-host species to *E. autumnata* (Ruohomäki et al., 2000) and is therefore not affected by its caterpillars. Yet, it should be taken into account that it reacts slightly differently to climatic influences than birch (Andreassen & Tomter, 2003).

2.4. Multi-evidence approach

For the assessment and reconstruction of *E. autumnata* outbreaks, five datasets were combined (Fig. 3). Digital change detection and historical documents cover five outbreak events back to 1955 (Tenow, 1972; Eckstein et al., 1991; Bylund, 1995; Karlsson et al., 2004) and serve as a validation for the tree-ring based detection of heavy defoliation. Detection in the 19th and early 20th century is based on a lowest 10th percentile threshold in three residual chronologies per site (B–T, B–R, B–P).

3. Results

3.1. Distribution of defoliation

Application of digital change detection allowed for the development of maps that show the relative damage distribution caused by caterpillars of *E. autumnata* during the three most recent outbreaks in 1986, 1994 and 2004. Previous investigations (e.g. Tømmervik et al., 2001) indicated that the largest NDVI decline coincided with the heaviest defoliation and the highest caterpillar density. This association was utilized here to produce damage maps, which were additionally verified by image differentiation on the equivalent multi-temporal image pairs. The relative classes of the 2004 event shown in Fig. 4 may therefore be assumed to correctly represent the severity of damage.

Results indicate that the damage pattern in 2004 was strongly dependant on topographical/artificial structures that influence moth dispersal. Mountain valleys appear to have been less affected than

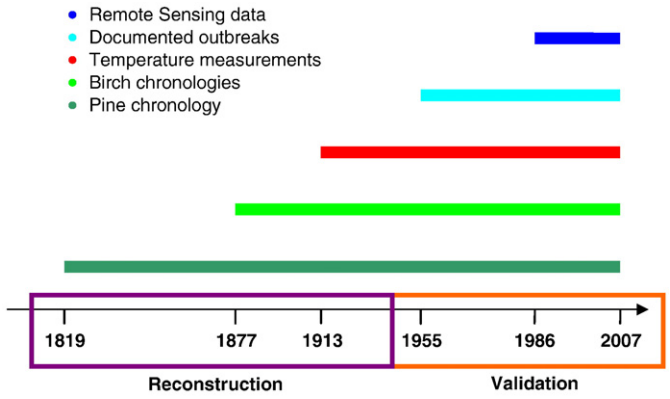

Fig. 3. Time periods covered by the five available data sources (multi-proxy approach). The years on the time axis indicate the beginning of a dataset. The longest birch chronology derives from T1_mid (1877–2007). The years covered by remotely sensed data and by historical records serve as a validation period for outbreak reconstruction prior to 1955.

low-elevation areas in the national park, as were most of the steep slopes on the north and south-west side of Lake Torneträsk. Extreme damage equals an NDVI decline >0.4 and only covers a very small area in the easternmost part of the research area. Severely defoliated areas were situated south of the lake and around its north-west end at low elevations and on slopes with moderate inclinations. Moreover, the forest distribution shows that the low average summer temperatures and the short growth period from June to August allow for tree growth in mountain valleys only on the south-facing valley slopes. The heath-type birch forest is not area-wide but interrupted by clearances, bogs and small lakes which have consequences for the dispersion of the poor-flying moths (Ruohomäki et al., 2000). The photo of T1 (Fig. 4) was taken in July 2004 at the stage of maximum defoliation. Intact parts of the forest are close to the treeline where the site T1_top is situated. This is clearly visible in both the map and the photo, which underlines the influence of topography.

The combination of digital change detection and tree-ring chronologies requires the assessment of defoliation on stand level. When spatial subsets covering T1 and T2 were selected from the change detections of 1986, 1994 and 2004, varying intensities of the most recent *Epirrita* population peaks became visible. Fig. 5 shows a

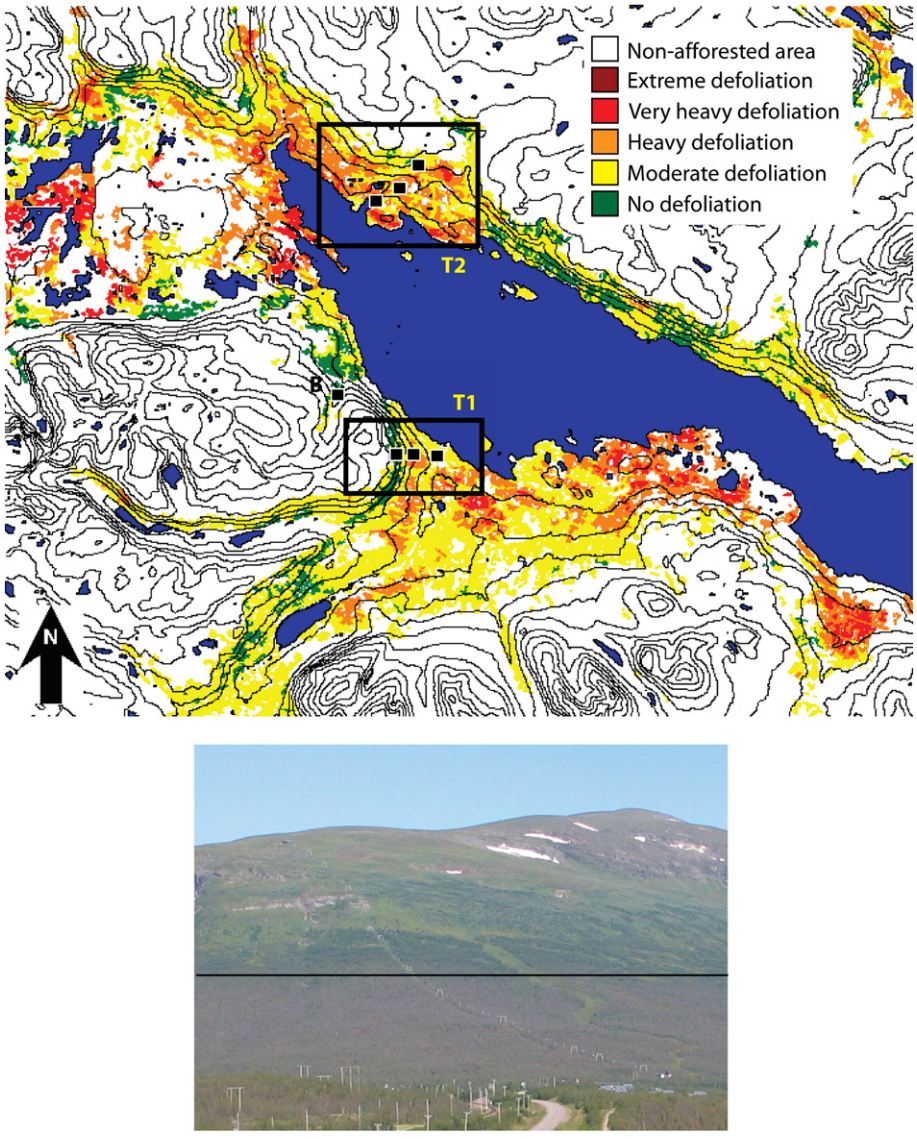

Fig. 4. Gap-filled damage distribution map of the research area showing the defoliation pattern during the 2004 outbreak. Black rectangles and dots indicate the location of the transects T1 and T2 as well as the birch reference site R. The adjacent picture shows the SE-facing slope (T1) during the 2004 event (08-02-2004). The black line indicates the border between defoliated mid-slope forest and undamaged stands close to treeline. This pattern is also clearly visible in the map.

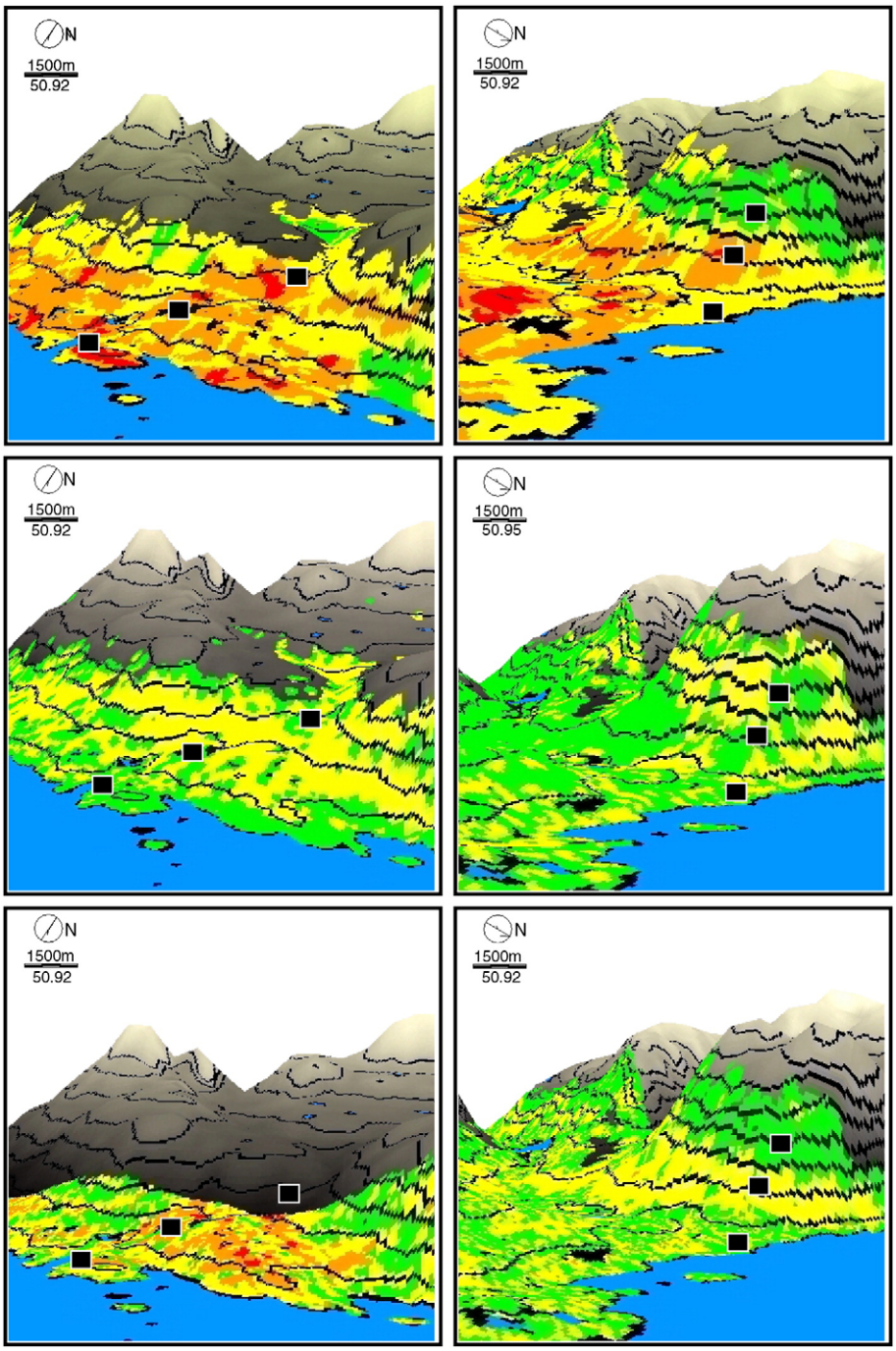

Fig. 5. 3-D view of defoliation classes along T1 (right column) and T2 (left column). Top row: 2004 outbreak (intense, covers both sides of Lake Torneträsk); middle row: 1994 event (slight defoliation, not detectable with dendrochronology); bottom row: 1986 incident (damage only along T2, T2_top not covered). The colour classes represent damage intensity: green equals no defoliation; yellow represents moderate defoliation; orange equals heavy defoliation; red stands for severe defoliation. (For interpretation of the references to colour in this figure legend, the reader is referred to the web version of this article.)

three-dimensional view of the damage classes along both transects with a vertical DEM exaggeration of factor five. This approach allows for altitudinal variations to be distinguished and directly related to the proxy data. A severe disturbance such as the 2004 event leads to a patchy distribution of heavily defoliated areas. In contrast, a less severe population peak like the one in 1994 only triggered moderate or no loss of foliage. The images also reveal that an outbreak does not necessarily occur on both sides of the lake as T2 showed damage in 1986, whereas T1 did not (bottom panels in Fig. 5). T2_top is not covered by the 1986 Landsat image. Along T1 but also to a certain degree along T2, the less defoliated forest areas are situated on the upper part of the slopes close to the treeline whereas heavier damage appears on the mid-slopes and partly the low-lands. This matches the photograph in Fig. 4.

3.2. Reconstruction

Correlations between JJA temperature and the defoliated sites T1_low and T1_mid are 0.39 and 0.45 respectively (1913–2007 period). The undisturbed site T1_top correlates more strongly with summer temperatures ($r = 0.67$). The sites along T2 reveal weaker correlations ($r = 0.27$ to 0.38).

Fig. 6 displays the B–T residuals for each site on both transects. On both sides of Lake Torneträsk, the low and mid-elevation sites react similarly to influences other than temperature, which is confirmed by the high correlation of the residuals at T1_low and T1_mid (0.82) as well as at T2_low and T2_mid (0.80). The mid-elevation sites appear to be slightly more affected by moth outbreaks than the lower sites. Stands close to the treeline, particularly the unaffected T1_top react differently, sometimes even oppositely ($r = 0.2$). These findings match the satellite-based damage distribution map (Figs. 4 and 5).

In all residual chronologies (B–T, B–R, B–P), heavy outbreaks appear either as single downward peaks or as prolonged sequences of negative values, thus indicating the defoliation event plus several recovery years (Tenow & Bylund, 2000). All values lower than the 10th percentile were retained as probable outbreak years. Strong positive residuals often occur in the years following severe defoliation. This was the case in the 1920s (T1), the late 1940s (T2), the early 1960s (T1), the late 1960s (T2) and in 2005/06 (T1). Two periods of positive anomalies in the late 1930s and the early 1980s, however, were not associated with defoliation.

All five data sources (change detection, historical records, temperature residuals, birch residuals and pine residuals) were combined in a multi-evidence reconstruction of *E. autumnata* outbreaks in the 19th and 20th centuries. Fig. 7 shows the reconstruction based on the longest site chronologies (T1_mid and T2_mid), which captured all events that were indicated by the other site chronologies. The probability of the correct detection of an outbreak increased with the number of available datasets indicating it. During the validation period (1955–2007), the two major events in 1955 and 2004 along T1 were detected by all available datasets, as was defoliation in 1955, 1965, 1986 and 2004 along T2. One known outbreak with a lower *Epirrita* population density along T1 in 1994 was confirmed by the change detection and historical records (Karlsson et al., 2004) but not captured by the tree-ring proxies. Altogether, the multi-proxy reconstruction detected a total of nine major insect outbreaks since 1820 which are listed in Table 3.

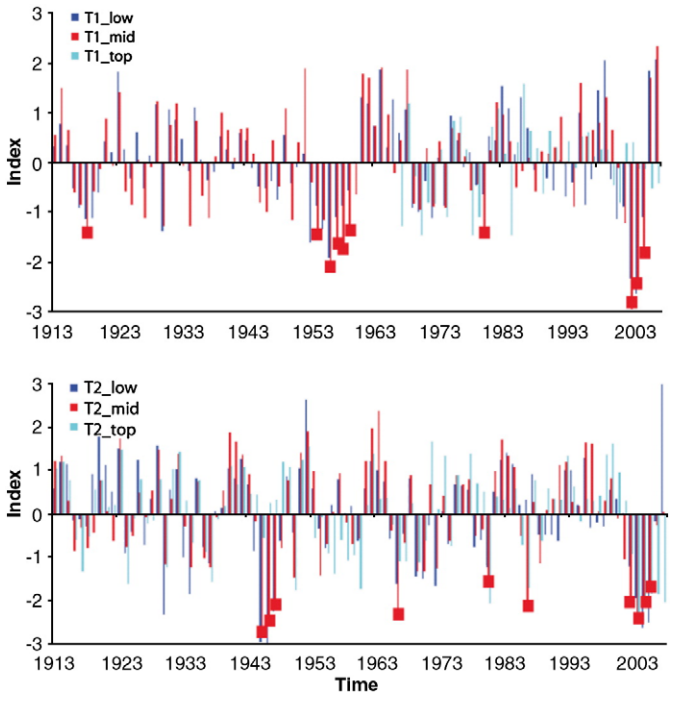

Fig. 6. Residuals between tree-ring width and standardized temperature measurements (ANS) at the sites along transects T1 (top) and T2 (bottom). Probable outbreaks and recovery periods are marked with red squares.

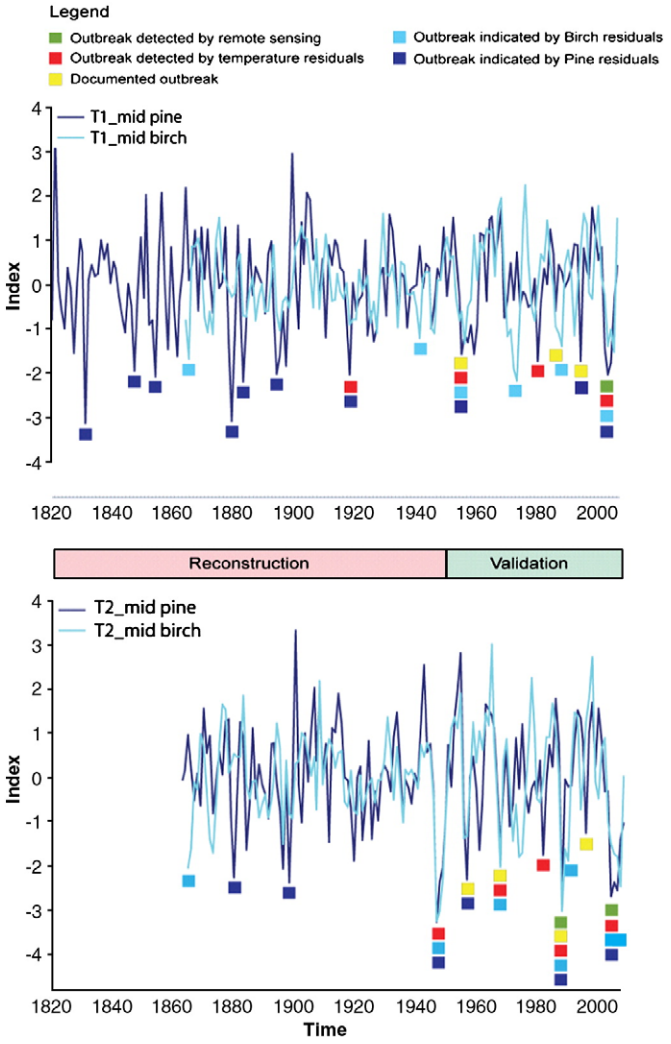

Fig. 7. Multi-proxy outbreak detection in recent and pre-measurement time (prior to 1913). Values lower than the 10th percentiles of each tree-ring proxy are marked as major outbreak events. The validation period for outbreak reconstruction is defined by the availability of satellite data and historical records (1955–2004). The variance has been checked in order to avoid biases due to a rapidly decreasing replication in the early 19th century.

3.3. Comparison of methods

A direct comparison of remote sensing with dendrochronology revealed a significant non-linear relationship ($r^2 = 0.64$, $p < 0.01$) between the decrease in standardized radial growth and the NDVI decline caused by an *E. autumnata* outbreak (Fig. 8). While the change

Table 3
Summary of major outbreak years detected by the five available datasets at the mid-sites of both transects (T1_mid, T2_mid).

Detected outbreak year	Number of available proxies indicating the incident in T1_mid (left column) T2_mid (right column)	
2004	4/4	4/4
1986	1/5	5/5
1965	0/4	¾
1955	3/4	2/4
1945	0/3	3/3
1918	2/3	0/3
1894	1/2	0/2
1879	1/2	½
1847	1/1	0/1

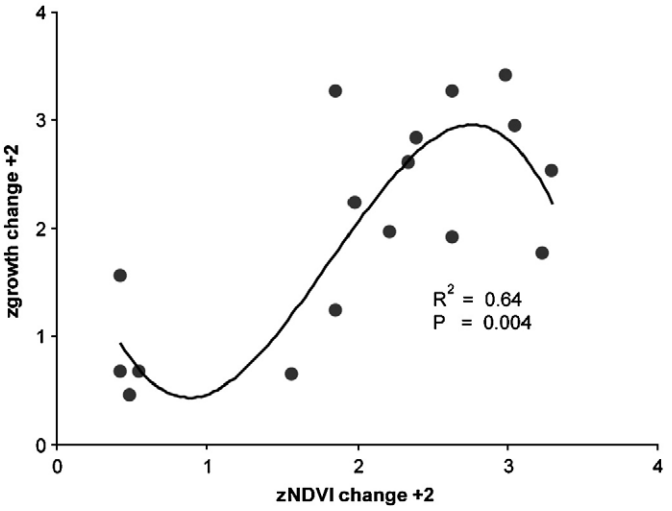

Fig. 8. Connection between standardized radial growth change and alteration of the standardized NDVI during *Epirrita autumnata* outbreaks. A 3rd degree polynomial regression revealed a significant non-linear relationship.

in the vegetation index is linear to the loss of leaf area, the radial growth reduction is not. This non-linearity matches the findings of Hoogesteger and Karlsson (1992) who revealed that defoliation up to 50% leaves no significant fingerprint in the wood whereas the annual ring width is dramatically reduced for one or several years if more than 80% of the foliage is devastated. Due to the small number of datapoints which are defined by the amount of available comparison sites, the polynomial regression line becomes unstable towards both ends. Furthermore, there is considerable scatter, the reasons for which will be discussed.

4. Discussion

Fine-spatial resolution NDVI-based digital change detection proved to be a useful tool to assess disturbances of the dominant mountain birch forest in northern Sweden. Since the vegetation distribution has not changed significantly over the period covered by satellite data (Masek, 2001), forest density and type played a key role in the reduction of the vegetation index due to *Epirrita*-caused defoliation. Earlier studies have shown that the abundance of host species and site ecology (e.g. soil moisture) have a significant influence on the cyclicities and patterns of Lepidoptera population peaks (Johnson et al., 2006; Haynes et al., 2009). Our change detection generally shows that dense mountain birch forests on mid-slopes are more severely damaged than those in flat, moist areas. This is confirmed by the finding of Johnson et al. (2006) who stated that outbreaks are more frequent at xeric sites compared to mesic sites. The present study was carried out over a limited area and large scale geographic variations (Haynes et al., 2009) in outbreaks may be neglected. Furthermore, the species composition may be described as monocultural (Vegetationskarta, 1981). Thus, the outbreak patterns are bound to be dependent on climate factors and population dynamics of *E. autumnata*. Another factor leading to more severe defoliation in mid-slope situations is the fact that the poor-flying female moths do not travel far and dispersal by ballooning is easier in close stands (Ruohomäki et al., 2000). As a consequence, light heath birch forest in flat areas are less accessible for *Epirrita* and NDVI reduction, which is potentially lessened by the unaffected photosynthesis performing undergrowth (Heiskanen, 2006), is therefore smaller.

Our results indicate that defoliation events and associated damage decrease from mid-slopes towards treeline and confirm the findings of Tenow (1972) and Bylund (1995). A comparison between slope angles (derived from the DEM) and defoliation detection revealed that steep slopes appear to be less affected than moderately inclined slopes, as are mountain valleys which usually establish an independent microclimate (Kirchhefer, 1996). Strong inclinations therefore appear to reduce or prevent an upward movement of *Epirrita*.

Damage detection of the 2004 outbreak reveals a patchy distribution of defoliation classes over the research area. The Abisko National Park prevents artificial clearcuts which therefore can be excluded as an explanation. It is likely that natural barriers like bogs, small lakes or hills (which are additionally inhabited by non-host tree species like *P. sylvestris*) preclude the moths from spreading equally over the area. Artificial structures which could have an equivalent effect on moth distribution are not present. Furthermore, the gap-fill process applied to the 2004 image may influence the result in terms of minor artifacts that were not entirely smoothed away by filter algorithms. Thus, the patchwork of damage classes may be locally enhanced where missing scan lines were located. This, however, does not affect the quality of the validation since the tree-ring sites represent a growth integral over several pixels.

The three-dimensional view created from the DEM (Fig. 5) allows for the visualization of damage-based change on the stand level. This application ensured comparability with ring-width data via geographic coordinates (GPS). For our research area, it seems unlikely that remotely sensed data with a higher spatial resolution than the one used in this study (30 m) would significantly improve this association in terms of the multi-proxy approach. The sampling sites measure approximately 150–200 m^2 depending on forest density. Therefore, the site chronologies represent a growth integral over a – in this case – monocultural forest area considerably larger than the current pixel size. Thus, an average value calculated from smaller pixels would not reflect tree growth better, nor would it justify the considerably larger amount of data (Townshend & Justice, 1988). If, however, insect outbreaks take place in mixed forests with co-dominant non-host species (e.g. Esper et al., 2007) the spatial resolution of Landsat provides a mixed NDVI signal from host and non-host individuals. In such cases, either a finer spatial resolution is required or the non-host signals have to be filtered out in order to ensure an accurate comparison between the vegetation index and ring-width data from disturbed trees.

A common disturbance signal in the different datasets is important for a robust reconstruction of outbreak events. Direct comparison between the change detection and three tree-ring proxies suggested that moderate defoliation does not necessarily leave a recognizable signal in the wood. Therefore, the low-intensity 1994 outbreak along T1 was not captured by two out of three residual chronologies. This is likely due to the non-linear relationship between loss of foliage and growth reduction (Hoogesteger & Karlsson, 1992). As a consequence, low to moderate *Epirrita* population peaks may only be detected with remote sensing techniques (or other methodologies), while dendrochronology allows for the quantification and reconstruction of severe outbreaks. Tree-ring residuals data are limited by the co-dependence to other disturbances and growing season temperatures (e.g. Büntgen et al., 2009; Esper et al., 2007; Frank et al., 2005). Thus, an outbreak during a cold summer is not reconstructable (Eckstein et al., 1991) unless stem mortality occurs over a large area in which case datable basal sprouts would be produced for survival (Kallio & Lehtonen, 1975). With the current methodology, it is impossible to distinguished between a narrow birch ring due to cold vegetation period temperatures, an insect outbreak, or both (which would likely cause a missing ring). Furthermore, the growth residuals between pine and birch are bound to be less negative in a cool growing season since both species react in a similar way to climate in the research area. An outbreak thus is not detected in a summer with distinct below average temperatures.

Outbreaks in the B–R residuals were detected back to 1940 only, which indicates that R probably belonged to the disturbed area prior to this date. This is evidence for a shift in the outbreak distribution in the middle of the 20th century. B–P residuals, on the other hand, detect outbreaks regularly back to 1820. The Scots pine chronology is therefore

considered to be a more reliable reference in pre-instrumental times since it is a non-host species (Ruohomäki and Haukioja, 1992) and thus guaranteed to be attack-free. Scots pine is also unlikely to strongly benefit from reduced light competition in an outbreak year since it only grows on dry hills in the flat areas of the Abisko National Park and is generally much taller than mountain birch.

The fact that affected sites react similarly, while the unaffected T1_top shows different or opposite residuals, serves as a validation for the change detection and confirms the influences of slope angle and elevation on the damage distribution. Along T2 which is on a moderately inclined slope, all sites were defoliated in 2004. Considering the different site properties within the transect, the correlations between the chronologies (T2_top – T2_mid: 0.66, T2_top – T2_low: 0.39) appear high. Thus, climate is likely to influence the annual radial growth much stronger than tree density and other site characteristics (Hjälten et al., 1993). Furthermore, the three most recent outbreaks underline that only the most severe events trigger defoliation on both sides of Lake Torneträsk under similar climatic conditions (Klemola et al., 2006). Temperature residuals indicated strong positive growth anomalies after most of the reconstructed disturbances. These could be caused by increased light availability and reduced competition after stem mortality (Eckstein et al., 1991), a heightened amount of nutrients or a potentially higher soil temperature due to more direct solar irradiation (Katan, 1981).

All five datasets available for analysis and reconstruction have their strengths and weaknesses. Remotely sensed data are area-wide and proved highly accurate for damage assessment. However, only the three most recent outbreaks are covered by Landsat imagery and only relative information about the *Epirrita*-caused damage is provided. Tree-ring data reach much further back in time and provide absolute radial growth reduction due to an event. Yet, tree-ring data are site-specific and unable to reflect outbreaks during cold summers. Furthermore, tree-ring analysis relies on the assumption that temperature, growth variability and insect-related disturbances are relevant growth determinants. This fully excludes precipitation which, in earlier studies, was found to have only a minor impact on the variance in detrended ring-width series (Eckstein et al., 1991). Thus, it appears reasonable that insect outbreaks account for the bigger part of the 20% variance that is not explained by temperature and growth variability (Karlsson et al., 2004).

Only the combined multi-proxy approach used in this study increases the accuracy and certainty of the outbreak detection. The proxy-based reconstruction is validated during the overlapping period with satellite data and historic documents from the research area. It became clear, however, that this method only allows for the reconstruction of severe defoliation events and provides no clear signals from low-intensity outbreaks. A 9 to 10 year cyclicity of *E. autumnata* population peaks in the middle of each decade over the 20th century was found in earlier investigations (Tenow, 1972; Bylund, 1995; Karlsson et al., 2004). Our outbreak reconstruction correctly assesses this cyclicity in the study area and detected severe defoliation events in 1945, 1955, 1965, 1986 and in 2004. The time period between 1918 and 1945 is known to be outbreak-free in the area of Lake Torneträsk (Tenow, 1972). Potential events in the mid 1970s and 1990s were not captured by our reconstruction. Summer 1975 was very cool (average temperatures were 2° below the 20th century average) which prevents detection by B–T and B–P residuals. The population peak in the mid 1990s is indicated by the satellite data. Likely, it was not severe enough to be detected with tree-ring methods.

A significant connection between NDVI decline and reduction in standardized radial growth due to an *Epirrita* outbreak was found. If further substantiated, it carries enormous potential since it allows for the extrapolation of in-situ derived measurements into a greater area and is a step into the direction of quantifying the loss of biomass due to insect outbreaks (e.g. Dong et al., 2003). Moreover, it is clearly related to regional climate change (frequency of egg-killing minimum winter temperatures) and may therefore become a bigger issue under a warming climate (Ruohomäki, 2000). The significant non-linear relationship presented in this study is not replicated well enough for application. The considerable scatter is likely to be caused by differing site properties such as forest density and photosynthetic activity of the undergrowth. This bias needs to be reduced in order to determine a robust relationship between reduction of NDVI and radial growth during an insect outbreak. Improved results may already be achieved by increasing the number of comparison sites. Despite the high variance of the presented data, the critical defoliation threshold of 80% (Hoogesteger & Karlsson, 1992) is correctly addressed. This may trigger further investigation into this matter.

5. Conclusions

Multispectral Landsat TM and ETM+ images are reliable for the detection of defoliation caused by *E. autumnata* using digital change detection. Damage was found to be dependant on topography, microclimate and vegetation type, as well as site conditions. All of these factors lead to a patchy dispersion of individual disturbance intensity classes. A multi-proxy approach based on remote sensing and dendrochronological techniques allowed for the detection and reconstruction of nine major insect outbreaks in the research area back to 1820. Defoliation did not necessarily occur on both sides of Lake Torneträsk which works as a natural barrier for moth distribution. Only the most severe outbreaks (1955 and 2004) triggered abnormal population growth on both shores while stands at higher altitudes and on steep slopes were least affected. The significant non-linear relation between NDVI reduction and the decrease in radial growth during an *Epirrita* outbreak allows – if further developed – for the extrapolation of in-situ measurements into a greater area.

Acknowledgements

The authors would like to thank the Swiss Academy of Sciences (SCNAT), the Swiss Federal Research Institute WSL and the Institute for Meteorology, Climatology and Remote Sensing of the University of Basel for their financial contributions. This work was also supported by the Swiss National Science Foundation through the National Centre for Competence in Climate Research (NCCR-Climate). Thanks to the Abisko Scientific Research Station (ANS Kiruna) for the preparation of climate data.

Special thanks to Rik van Bogaert, Dieter Eckstein and Jan Hoogesteger for their useful data contributions. Furthermore, we thank Valerie Trouet for the detailed corrections to the manuscript. Thanks to Günter Bing, Corinne Frey, David Frank, Ulf Büntgen, and Daniel Nievergelt for their help and the fruitful discussions.

References

Andreassen, K., & Tomter, S. M. (2003). Basal area growth models for individual trees of Norway spruce, Scots pine, birch and other broadleaves in Norway. *Forest Ecology and Management*, *180*, 11—24.

Büntgen, U., Frank, D., Liebhold, A., Carrer, M., Urbinati, C., Grabner, M., et al. (2009). Three centuries of insect outbreaks across the European Alps. *New Phytologist*, *182*, 929—941.

Bylund, H. (1995). Long-term interactions between the autumnal moth and mountain birch — the roles of resources, competitors, natural enemies and weather. In F. E. Wielgolaski (Ed.), *Nordic mountain birch ecosystems* (pp. 1—390). UNESCO.

Bylund, H. (1997). Stand age–structure influence in a low population peak of *Epirrita autumnata* in a mountain birch forest. *Ecography*, *20*, 319—326.

Cook, E. R., & Holmes, R. L. (1986). Program ARSTAN — Chronology development, statistical analysis. Laboratory of TreeRing Research, University of Arizona, 50—65.

Cook, E. R., & Peters, K. (1981). The smoothing spline: A new approach to standardizing forest interior tree-ring width series for dendroclimatic studies. *Tree-Ring Bulletin*, *41*, 45—53.

Cook, E. R., & Peters, K. (1997). Calculating unbiased tree-ring indices for the study of climatic and environmental change. *Holocene*, *7*(3), 361—370.

Coppin, P., Lambin, E., Jonckheere, I., & Muys, B. (2002). Digital change detection methods in natural ecosystem monitoring — A review. In L. Bruzzone & P. Smits (Eds.), *Analysis of multi-temporal remote sensing images* (pp. 1—430). World Scientific.

Dong, J., Kaufmann, R., Myneni, R., Tucker, C., Kauppi, P., Liski, J., et al. (2003). Remote sensing estimates of boreal and temperate forest woody biomass: carbon pools, sources and sinks. *Remote Sensing of Environment*, *84*, 393—410.
Eastman, J. R., & Fulk, M. (1993). Long sequence time series evaluation using standardized principal components. In J. R. Jensen (Ed.), *Introductory Digital Image Processing* (pp. 1—526). Prentice Hall.
Eckstein, D., Hoogesteger, J., & Holmes, R. L. (1991). Insect-related differences in growth of birch and pine at northern treeline in Swedish Lapland. *Holarctic Ecology*, *14*(1), 18—23.
Eklundh, L., Johansson, T., & Solberg, S. (2009). Mapping insect defoliation in Scots pine with MODIS time-series data. *Remote Sensing of Environment*, *113*, 1566—1573.
Eschbach, W., Nogler, P., Schär, E., & Schweingruber, F. H. (1995). Technical advances in the radiodensitometrical determination of wood density. *Dendrochronologia*, *13*, 155—168.
Esper, J., & Schweingruber, F. H. (2004). Large-scale treeline changes recorded in Siberia. *Geophysical Research Letters*, *31*, L06202.
Esper, J., Büntgen, U., Frank, D. C., Nievergelt, D., & Liebhold, A. (2007). 1200 years of regular outbreaks in alpine insects. *Proceedings of the Royal Society B*, *274*, 671—679.
Frank, D. C., Esper, J., & Cook, E. R. (2007). Adjustment for proxy number and coherence in large-scale temperature reconstructions. *Geophysical Research Letters*, *34*, L16709.
Frank, D. C., Wilson, R., & Esper, J. (2005). Synchronous variability changes in Alpine temperature and tree-ring data over the past two centuries. *Boreas*, *34*, 498—505.
Franklin, S. E., & Raske, A. G. (1994). Satellite remote sensing of spruce budworm forest defoliation in western Newfoundland. *Canadian Journal of Remote Sensing*, *20*, 37—48.
Fraser, R. H., Abulegasim, A., & Latifovic, R. (2005). A method for detecting large-scale forest cover change using coarse spatial resolution imagery. *Remote Sensing of Environment*, *95*, 414—427.
Fritts, H. C. (1976). Tree rings and climate. The Blackburn Press, 1—567.
Goward, S. N., Davis, P. E., Fleming, D., Miller, L., & Townsend, J. R. (2003). Empirical comparison of Landsat 7 and IKONOS multispectral measurements for selected Earth Observation System (EOS) validation sites. *Remote Sensing of Environment*, *112*, 2367—2380.
Haynes, K. J., Liebhold, A. M., & Johnson, D. M. (2009). Spatial analysis of harmonic oscillation of gypsy moth outbreak intensity. *Oecologia*, *159*, 249—256.
Heiskanen, J. (2006). Estimating aboveground tree biomass and leaf area index in a mountain birch forest using ASTER satellite data. *International Journal of Remote Sensing*, *27*(6), 1135—1158.
Heiskanen, J., & Kivinen, S. (2007). Assessment of multispectral, -temporal and -angular MODIS data for tree cover mapping in the tundra–taiga transition zone. *Ecology*, *74*(4), 1136—1142.
Hjälten, J., Danell, K., & Ericson, L. (1993). Effects of simulated herbivory and intraspecific competition on the compensatory ability of birches. *Remote Sensing of Environment*, *112*(5), 2367—2380.
Hogda, K. A., & Tommervik, H. (1998). Detection of caterpillar outbreaks in mountain birch forests. *27th international symposium on remote sensing, proceedings — Information for sustainability* (pp. 532—534)..
Holben, B., & Justice, Ch. (1981). An examination of spectral band ratioing to reduce the topographic effect on remotely sensed data. *International Journal of Remote Sensing*, *2*(2), 115—133.
Holmes, R. L. (1983). Computer-assisted quality control in treering dating and measurement. *Tree-Ring Bulletin*, *43*, 69—78.
Hoogesteger, J., & Karlsson, P. S. (1992). Effects of defoliation on radial stem growth and photosynthesis in the mountain birch (*Betula pubescens* ssp. tortuosa). *Functional Ecology*, *6*(3), 317—323.
Jensen, J. R. (2005). Introductory digital image processing. Prentice Hall.
Jepsen, J. U., Hagen, S. B., Ims, R. A., & Yoccoz, N. G. (2008). Climate change and outbreaks of the geometrids *Operophtera brumata* and *Epirrita autumnata* in subarctic birch forests — Evidence of a recent outbreak range expansion. *Journal of Animal Ecology*, *77*(2), 257—264.
Jin, S., & Sader, S. A. (2005). MODIS time-series imagery for forest disturbance detection and quantification of patch size effects. *Remote Sensing of Environment*, *99*, 462—470.
Johnson, D. M., Liebhold, A. M., & Bjornstad, O. N. (2006). Geographical variation in the periodicity of gypsy moth outbreaks. *Ecography*, *29*, 367—374.
Kallio, P., & Lehtonen, J. (1975). On the ecocatastrophe of birch forests caused by *Oporinia autumnata* (Bkh.) and the problem of reforestation. In F. E. Wielgolaski (Ed.), *Fennoscandian tundra ecosystemsEcological studies*, *vol. 17* (pp. 174—180).
Karlsson, P. S., Tenow, O., Bylund, H., Hoogesteger, J., & Weih, M. (2004). Determinants of mountain birch growth in situ: Effects of temperature and herbivory. *Ecography*, *27*, 659—667.
Katan, J. (1981). Solar heating (solarization) of soil for control of soilborne pests. *Annual Review of Phytopathology*, *19*, 211—236.
Kirchhefer, A. J. (1996). A dendrochronological study on the effect of climate, site and insect outbreaks on the growth of *Betula pubescens* coll. in northern Norway. *Paleoclimate Research*, *20*, 93—106.
Klemola, T., Huitu, O., & Ruohomäki, K. (2006). Geographically partitioned spatial synchrony among cyclic moth populations. *Oikos*, *114*, 349—359.
Leckie, D. G., Cloney, E., & Joyce, S. P. (2005). Automated detection and mapping of crown discolouration caused by jack pine budworm with 2.5 m resolution multispectral imagery. *Journal of Applied Earth Observation and Geoinformation*, *7*, 61—77.
Li, X., & Yeh, A. G. O. (1998). Principal component analysis of stacked multi-temporal images for the monitoring of rapid urban expansion in the Pearl River Delta. *International Journal of Remote Sensing*, *19*(8), 1501—1518.
Lu, D., Mausel, P., Brondizio, E., & Moran, E. (2004). Change detection techniques. *International Journal of Remote Sensing*, *25*(12), 2365—2401.
Masek, J. G. (2001). Stability of boreal forest stands during recent climate change — Evidence from Landsat satellite imagery. *Journal of Biogeography*, *28*, 967—976.
Maxwell, K. S., Schmidt, G. L., & Store, J. C. (2007). A multi-scale segmentation approach to filling gaps in Landsat ETM+ SLC-off images. *International Journal of Remote Sensing*, *28/23*, 5339—5356.
Parlow, E. (1985). LANDSAT-Thematic Mapper and SPOT – Fernerkundungssatelliten der 2. Generation. *Geographische Rundschau*, *37*(4), 194—198.
Radeloff, V. C., Mladenoff, D. J., & Boyce, M. S. (1999). Detecting jack pine budworm defoliation using spectral mixture analysis: Separating effects from determinants. *Remote Sensing of Environment*, *69*, 156—169.
Radeloff, V. C., Mladenoff, D. J., & Boyce, M. S. (2000). Effects of interacting disturbances on landscape patterns: Budworm defoliation and salvage logging. *Ecological Applications*, *10*, 233—247.
Remmel, T. K., & Perera, A. H. (2001). Fire mapping in a northern boreal forest — Assessing AVHRR/NDVI methods of change detection. *Forest Ecology and Management*, *152*, 119—129.
Richards, J. A., & Xiuping, J. (1999). Remote sensing digital image analysis. Springer, 1—363.
Rogan, J., Franklin, J., & Roberts, D. (2002). A comparison of methods for monitoring multitemporal vegetation change using Thematic Mapper imagery. *Remote Sensing of Environment*, *80*, 143—156.
Ruohomäki, K., & Haukioja, E. (1992). Interpopulation differences in pupal size and fecundity are not associated with occurrence of outbreaks in *Epirrita autumnata* (Lepidoptera, Geometridae). *Ecological Entomology*, *17*, 69–75.
Ruohomäki, K., Tanhuanpää, M., Ayres, M. P., Kaitaniemi, P., Tammaru, T., & Haukioja, E. (2000). Causes of cyclicity of *Epirrita autumnata* (Lepidoptera, Geometridae) — Grandiose theory and tedious practice. *Population Ecology*, *42*, 211—223.
Schweingruber, F. H. (1988). Tree rings — Basics and applications of dendrochronology. Reidel, 1—275.
Seppälä, M., & Rastas, J. (1980). Vegetation map of northernmost Finland with special reference to subarctic forest limits and natural hazards. In F. E. Wielgolaski, P. S. Karlsson, S. Neuvonen, & D. Thannheiser (Eds.), *Plant ecology, herbivory and human impact in nordic mountain birch forestsEcological Studies*, *vol. 180* (pp. 1—365).
Solberg, S., Nasset, E., Hanssen, K. H., & Christiansen, E. (2006). Mapping defoliation during a severe insect attack on Scots pine using airborne laser scanning. *Remote Sensing of Environment*, *102*, 364—376.
Stow, D. A., Hope, A., McGuire, D., Verbyla, D., Gamon, J., Huemmrich, F., et al. (2004). Remote sensing of vegetation and land-cover change in arctic tundra ecosystems. *Remote Sensing of Environment*, *89*, 281—308.
Song, C., Woodstock, C., Seto, K., Lenney, M., & Macomber, S. (2001). Classification and change detection using Landsat TM data: When and how to correct atmospheric effects? *Remote Sensing of Environment*, *75*, 230—244.
Takaoka, S. (1993). The effect of missing rings on stand-age estimation of even-aged forests in northern Hokkaido, Japan. *Ecological Research*, *8*(3), 341—347.
Tenow, O. (1972). The outbreaks of *Oporinia autumnata* Bkh. and *Operophtera* spp. (Lep., Geometridae) in the Scandinavian mountain chain and northern Finland 1862–1968. PhD thesis Uppsala, 1–105.
Tenow, O., & Bylund, H. (2000). Recovery of a *Betula pubescens* forest in northern Sweden after severe defoliation by *Epirrita autumnata*. *Journal of Vegetation Science*, *11*(6), 855—862.
Tenow, O., Bylund, H., Karlsson, P. S., & Hoogesteger, J. (2004). Rejuvenation of a mountain birch forest by an *Epirrita autumnata* (Lepidoptera: Geometridae) outbreak. *Acta Oecologica*, *25*, 43—52.
Tenow, O., & Nilssen, A. (1990). Egg cold hardiness and topoclimatic limitations to outbreaks of *Epirrita autumnata* in northern Fennoscandia. *Journal of Applied Ecology*, *27*(2), 723—734.
Tømmervik, H., Høgda, K. A., & Karlsen, S. R. (2001). Using remote sensing for detection of caterpillar outbreaks in mountain birch forests — A new interesting approach. In F. E. Wielgolaski (Ed.), *2001: Nordic mountain birch ecosystems* (pp. 1—390). UNESCO.
Townsend, P. A., Eshleman, K. N., & Welcker, C. (2004). Remote sensing of gypsy moth defoliation to assess variations in stream nitrogen concentrations. *Ecological Applications*, *14*, 504—516.
Townshend, J. R. G., & Justice, C. O. (1988). Selcting the spatial resolutions of satellite sensors required for global monitoring of land transformations. *International Journal of Remote Sensing*, *9*(2), 187—236.
Trigg, S. N., Curran, L. M., & McDonald, A. K. (2006). Utility of Landsat 7 satellite data for continued monitoring of forest cover change in protected areas in Southeast Asia. *Singapore Journal of Tropical Geography*, *27*, 49—66.
Vegetationskarta over de Svenska Fjällen (1981, 1:100,000) – Kartblad nr 2: Abisko. LiberKartor Stockholm.
Virtanen, T., Neuvonen, S., & Nikula, A. (1998). Modelling topoclimatic patterns of egg mortality of *Epirrita autumnata* (Lepidoptera: Geometridae) with a Geographical Information System — predictions for current climate and warmer climate scenarios. *Journal of Applied Ecology*, *35*(2), 311—322.
Wigley, T. M. L., Briffa, K. R., & Jones, P. D. (1984). On the average of value of correlated time series, with applications in dendroclimatology and hydrometeorology. *Journal of Climatology and Applied Meteorology*, *23*, 201—213.
Williams, J. (1995). Geographic information from space — processing and applications of geocoded satellite images. Wiley, 1—210.
Wulder, M. A., Dymond, C. C., White, J. C., Leckie, D. G., & Carroll, A. L. (2006). Surveying mountain pine beetle damage of forests: A review of remote sensing opportunities. *Forest Ecology and Management*, *221*, 27—41.
Wulder, M. A., Skakun, R. S., Kurz, W. A., & White, J. C. (2004). Estimating time since forest harvest using segmented Landsat ETM+ imagery. *Remote Sensing of Environment*, *93*, 179—187.